

See discussions, stats, and author profiles for this publication at: <https://www.researchgate.net/publication/261328649>

# WIN induces apoptotic cell death in human colon cancer cells through a block of autophagic flux dependent on PPAR $\gamma$ down-regulation

ARTICLE *in* APOPTOSIS · APRIL 2014

Impact Factor: 3.69 · DOI: 10.1007/s10495-014-0985-0 · Source: PubMed

CITATION

1

READS

50

## 7 AUTHORS, INCLUDING:



**Ornella Pellerito**

Laval University

14 PUBLICATIONS 176 CITATIONS

SEE PROFILE



**Antonietta Notaro**

Università degli Studi di Palermo

6 PUBLICATIONS 25 CITATIONS

SEE PROFILE



**Selenia Sabella**

Università degli Studi di Palermo

4 PUBLICATIONS 14 CITATIONS

SEE PROFILE



**Michela Giuliano**

Università degli Studi di Palermo

55 PUBLICATIONS 894 CITATIONS

SEE PROFILE

# WIN induces apoptotic cell death in human colon cancer cells through a block of autophagic flux dependent on PPAR $\gamma$ down-regulation

Ornella Pellerito · Antonietta Notaro ·  
Selenia Sabella · Anna De Blasio · Renza Vento ·  
Giuseppe Calvaruso · Michela Giuliano

© Springer Science+Business Media New York 2014

**Abstract** Cannabinoids have been reported to possess anti-tumorigenic activity in cancer models although their mechanism of action is not well understood. Here, we show that the synthetic cannabinoid WIN55,212-2 (WIN)-induced apoptosis in colon cancer cell lines is accompanied by endoplasmic reticulum stress induction. The formation of acidic vacuoles and the increase in LC3-II protein indicated the involvement of autophagic process which seemed to play a pro-survival role against the cytotoxic effects of the drug. However, the enhanced lysosomal membrane permeabilization (LMP) blocked the autophagic flux after the formation of autophagosomes as demonstrated by the accumulation of p62 and LC3, two markers of autophagic degradation. Data also provided evidence for a role for nuclear receptor peroxisome proliferator-activated receptor  $\gamma$  (PPAR $\gamma$ ) in cannabinoid signalling.

PPAR $\gamma$  expression, at both protein and mRNA levels, was significantly down-regulated after WIN treatment and its inhibition, either by specific antagonists or by down-regulation via gene silencing, induced effects on cell viability as well as on ER stress and autophagic markers similar to those obtained in the presence of WIN. Moreover, the observation that the increase in p62 level and the induction of LMP were also modified by PPAR $\gamma$  antagonists seemed to indicate that PPAR $\gamma$  down-regulation was crucial to determinate the block of autophagic flux, thus confirming the critical role of PPAR $\gamma$  in WIN action. In conclusion, at our knowledge, our results are the first to show that the reduction of PPAR $\gamma$  levels contributes to WIN-induced colon carcinoma cell death by blocking the pro-survival autophagic response of cells.

**Keywords** Cannabinoids · PPAR $\gamma$  · ER stress · Autophagy/apoptosis interplay · Colon carcinoma cells

O. Pellerito and A. Notaro have contributed equally to this study. G. Calvaruso and M. Giuliano share senior co-authorship.

**Electronic supplementary material** The online version of this article (doi:10.1007/s10495-014-0985-0) contains supplementary material, which is available to authorized users.

O. Pellerito  
Laboratory of Cellular and Developmental Genetics, Department of Molecular Biology, Medical Biochemistry and Pathology, Faculty of Medicine, PROTEO and IBIS, Université Laval, Quebec, QC, Canada

A. Notaro · S. Sabella · A. De Blasio · R. Vento · G. Calvaruso · M. Giuliano (✉)  
Dipartimento STEBICEF Scienze e Tecnologie biologiche, chimiche e farmaceutiche, Laboratorio di Biochimica, Università di Palermo, Policlinico Universitario, Via del Vespro 129, 90127 Palermo, Italy  
e-mail: michela.giuliano@unipa.it

## Abbreviations

ER	Endoplasmic reticulum
PPAR $\gamma$	Peroxisome proliferator-activated receptor $\gamma$
CHOP	CCAAT/enhancer binding protein homologous protein
GRP78	Glucose-regulated protein 78/Binding immunoglobulin protein
TRB3	Tribbles-related protein 3
LC3 (MAP1LC3)	Microtubule-associated protein 1 light chain 3
PARP	Poly-(ADP-ribose) polymerase
WIN	(WIN55,212-2) R-[2,3-dihydro-5-methyl-3[(4-morpholinyl)methyl] pyrrolo[1,2,3,-de]-1,4-benzoxazin-6-yl]-1-naphthalenyl methanone mesylate

MTT	3-(4,5)-Dimethylthiaziazol(-z-y1)-3,5-diphenyltetrazoliummide
MDC	Monodansylcadaverine
PI	Propidium iodide
3-MA	3-Methyladenine
AO	Acridine orange
CCCP	Carbonylcyanide m-chlorophenylhydrazone
LMP	Lysosomal membrane permeabilization
Baf A1	Bafilomycin A1

## Introduction

Cannabinoids represent a class of chemical compounds that include the active constituents of *Cannabis sativa*, endocannabinoids, and the synthetic ligands of cannabinoid receptors [1]. It has been demonstrated that cannabinoids exert a wide range of central and peripheral effects after interaction with the specific cannabinoid receptors (CB1 and CB2), both of which belong to the G-protein-coupled receptor family. The CB1 subtype receptor is mainly expressed in the central nervous system, while the CB2 receptor is expressed in peripheral and immune tissues [2, 3]. Moreover, cannabinoids can also act via transient activated vanilloid receptors (TRPV1) or membrane microdomains rich in cholesterol, named lipid rafts [4, 5].

Numerous studies provided evidence for the role of cannabinoids in the regulation of cell survival and cell death, including anti-proliferative effects on tumor growth attributable to cannabinoid exposure in breast and prostate cancer, pheochromocytoma, and malignant gliomas [6–10]. The mechanisms by which cannabinoids exert antitumor effects include growth arrest, induction of cell death, and inhibition of tumor angiogenesis and metastasis [11]. In addition to the canonical apoptotic pathway, recent researches indicate that both natural and synthetic cannabinoids can induce the endoplasmic reticulum (ER) stress response accompanied by type II programmed cell death (autophagy) [12].

Autophagy is a process which was initially identified as a pro-survival mechanism that permits the turnover of cytoplasmic components or the recycling of degraded macromolecules in stressed cells. During the process, a membrane trafficking pathway delivers to the formation of the autophagosome which fuses with the lysosomes for protein degradation. It has been demonstrated the relationship between ER stress and induction of autophagy [13]. Under ER stress conditions some autophagy-related (ATG) family members are transcriptionally induced [14] and the conversion of LC3, a protein involved in

autophagosome formation, from LC3-I to -II can be facilitated [15]. Moreover, it has recently been demonstrated that cannabinoids modulate their cytotoxic action through ER stress-related pathway that promotes autophagy via TRB3-dependent inhibition of AKT [16].

In some experimental conditions, the autophagic process can be blocked by a number of stressors which target lysosomes and induce lysosomal membrane permeabilization (LMP) [17]. The consequences of this event are the inhibition of autophagosome acidification with the blocking of autophagy and/or the release of lysosomal proteases in the cytosol with the consequent triggering of cell death. The level of lysosomal damage will determine what death process (necrosis or apoptosis) will be activated in the cell.

Peroxisome proliferator-activated receptor  $\gamma$  (PPAR $\gamma$ ) is a ligand-activated transcription factor of the nuclear hormone receptor superfamily which is highly expressed in adipose tissue where it is considered a master regulator of adipocyte differentiation [18, 19]. PPAR $\gamma$  is also present in other tissues, such as breast, colon, lung, ovary, prostate and thyroid wherein it mediates several specific functions such as early development, cell proliferation, differentiation, apoptosis, and metabolic homeostasis [20, 21].

Many investigators have reported that PPAR $\gamma$  is also involved in the control of malignant cell growth since its activation by specific agonists inhibited cell proliferation, promoted differentiation, and induced apoptosis in a variety of malignant tissue types [22, 23]. However, although there is evidence that PPAR $\gamma$  acts as a tumor suppressor in various cancer types, other studies have indicated that in some human carcinoma cells PPAR $\gamma$  can also act as a tumor promoter when highly expressed [24]. The different behaviour of PPAR $\gamma$  seems to be related to cell type as well as the tumor grading or differentiation stage. Consequently, the function of PPAR $\gamma$  activating ligands as well as antagonists in cancer cell treatment remains controversial.

Recently, we and others have demonstrated a relationship between the cannabinoid system and the transcription factor PPAR $\gamma$  [25, 26]. We found that in hepatocellular carcinoma cells, WIN55,212-2 (WIN), a potent synthetic ligand of cannabinoid receptors, induced apoptosis with a substantial increase in the level of PPAR $\gamma$  which preceded the cytotoxic effect of the drug. Moreover, the addition of specific PPAR $\gamma$  antagonists markedly counteracted WIN cytotoxicity [25].

The aim of the present study was to investigate the effects of WIN treatment on colon cancer cells and the potential role of PPAR $\gamma$  in mediating WIN action. We demonstrated that in these cells, WIN induced a marked reduction in PPAR $\gamma$  level which caused induction of ER stress and was responsible for a block of autophagic flux with the consequent induction of apoptotic colon cancer cell death.

## Materials and methods

### Reagents

R-[2,3-dihydro-5-methyl-3[(4-morpholinyl)methyl] pyrrolo[1,2,3,-de]-1,4-benzoxazin-6-yl]-1-naphthalenyl methanone mesylate (WIN55,212-2), GW9662 and 3-methyladenine (3-MA) were purchased from Sigma-Aldrich, (MI, Italy); T0070907 (T007) was from Cayman Chemical (USA) and bafilomycin A1 from BioVotica (Vinci-Biochem, Firenze, Italy). Stock solutions were prepared in DMSO and opportunistically diluted in culture medium except for 3-MA which was prepared in ethanol. The final concentration of DMSO never exceeded 0.1 %, which is a concentration that was experimentally determined to have no discernible effect. Antibodies used were: against PPAR $\gamma$ , JunD, Fos, YY1, Notch1, GRP78, CHOP, TRB3 and pAKT from Santa Cruz Bio (CA, USA); against procaspase-3, -9, PARP and Beclin-1 from Cell Signaling (Beverly, MA, USA); against p62 and Actin from Sigma (MI, Italy); against LC3 from Novus Biologicals (Cambridge, UK).

### Cell cultures

Human colon cancer HT29, HCT116 and Caco-2 cells were cultured at 37 °C in RPMI 1640 medium (HT29 cells) or Dulbecco's Modified Eagle's Medium (DMEM) supplemented with 10 % (v/v) heat-inactivated foetal bovine serum (FBS), 2.0 mM L-glutamine, and antibiotic, antimycotic solution (100 U/ml penicillin, 100  $\mu$ g/ml streptomycin and 250 ng/ml amphotericin B, Sigma) in a humidified atmosphere containing 5 % CO<sub>2</sub>. For the experiments, cells were seeded at 60–70 % confluence. After overnight incubation, culture medium was replaced with fresh medium containing reduced FBS (2 %) and cells were treated with the compounds. Control cells were cultured in the presence of vehicle alone.

### MTT assay

3-[4,5-dimethylthiazolyl-2] 2,5-diphenyl-tetrazolium bromide (MTT) assay was employed to evaluate cell viability as previously reported [27]. Briefly, after treatment in 96-well plates, MTT stock solution was added to each well (final concentration 1 mg/ml) for 2 h. The medium was then removed and lysis buffer (0.1 ml) was added to dissolve the formazan product. Finally, the absorbance at 570 nm (test wavelength) and at 630 nm (reference wavelength) was measured using an ELISA microplate reader (Dynex Technologies). Data reported in the figures are the means  $\pm$  SD of four independent experiments involving triplicate assays.

### Cytofluorimetric analysis

For these assays was employed an Epics XL flow cytometer (Beckman Coulter) equipped with a single Argon ion laser (emission wavelength of 488 nm) and Expo32 software.

### Viability assay

Loss of cell viability was assessed by staining with propidium iodide (PI), a membrane impermeant dye which is generally excluded from viable cells. Cells were harvested, washed with phosphate-buffered saline (PBS) and incubated for 10 min at 4 °C in a solution of PBS containing 2  $\mu$ g/ml PI. After staining red fluorescence was measured in the FL3 channel using a 620-nm BP filter. Data reported in the figures are the means  $\pm$  SD of four independent experiments.

### Cell cycle analysis

To analyse cell cycle distribution, cells were harvested by trypsinization and resuspended in a hypotonic solution containing 50  $\mu$ g/ml propidium iodide, 0.1 % sodium citrate, 0.01 % Nonidet P-40 and 10  $\mu$ g/ml RNase A. The red fluorescence was measured in the FL3 channel using a 620-nm BP filter. Cell debris and aggregates were excluded by opportune gating and 5,000 events/sample were analysed. The percentage of cells in subG0/G1 phase was considered as an index of DNA fragmentation. The results showed in the figures are representative of four independent experiments.

### Measurement of mitochondrial transmembrane potential ( $\Delta\psi_m$ )

Mitochondrial transmembrane potential ( $\Delta\psi_m$ ) dissipation was measured as previously reported [28] using 3,3-dihexyloxycarbocyanine (DiOC6, Cayman Chemical, USA), a fluorochrome which exclusively emits within the spectrum of green light and accumulates in the mitochondrial matrix under the influence of  $\Delta\psi_m$ . The percentage of cells showing a lower fluorescence, reflecting the loss of  $\Delta\psi_m$ , was determined by comparison with untreated controls. The green fluorescence was measured in the FL1 channel using a 515-nm BP filter. Carbonylcyanide m-chlorophenylhydrazone (CCCP; 50  $\mu$ M), a protonophore that completely de-energises mitochondria by dissipating the transmembrane potential, was used as a positive control for maximum  $\Delta\psi_m$  disruption (Supplementary Fig. S1). The results showed in the figures are representative of four independent experiments.

### Measurement of lysosomal membrane integrity

LMP was assayed with the acridine orange (AO) uptake technique as previously described [29]. AO, a metachromatic fluorophore, accumulates mainly in the acidic vacuolar apparatus, preferentially in secondary lysosomes. When excited by blue light (relocation method) it shows red and green fluorescence at high (lysosomal) or low (nuclear and cytosolic) concentration, respectively. Rupture of initially acridine orange-loaded lysosomes may be monitored as an increase in cytoplasmic diffuse green, or a decrease in granular red, fluorescence [30]. For the experiments, cells ( $2 \times 10^5/2$  ml) were stained with AO (5  $\mu\text{g}/\text{ml}$ ) in culture medium for 15 min at 37 °C. Cells were then washed and exposed to drugs in complete medium. At the end of exposure, cells were resuspended in PBS and the cytosolic green fluorescence of 10,000 cells per sample was determined. The green fluorescence was measured in the FL1 channel using a 515-nm BP filter. Using this technique early alterations of lysosomal stability were assayed. All steps were carried out in the dark. Results are representative of four independent experiments.

### Fluorescence microscopy analysis

#### *Monodansylcadaverine (MDC) labeling*

MDC staining of autophagic vacuoles was used for autophagy analysis. After treatment on 96 well plates, cells were washed with PBS and stained with 0.05 mM MDC in PBS at 37 °C for 10 min. Following incubation, cells were washed three times with PBS and immediately analyzed under a fluorescence microscope. Images were photographed and captured by a computer-imaging system (Leica DC300F camera and Adobe Photoshop for image analysis).

#### *Acridine orange staining*

For qualitative evaluation of lysosomal membrane permeabilization, the cells were stained with the acridine orange (AO) as above described, cytospun and viewed on glass coverslips under a Leica DM IRB inverted microscope (Leica Microsystems Srl, Milano, Italy) equipped with epifluorescence optics and suitable filters for FITC and rhodamine detection. Images were photographed and captured by a computer-imaging system (Leica DC300F camera and Adobe Photoshop for image analysis).

### Immunoblotting analysis

Protein extracts were prepared by washing the cells in PBS and incubating for 20 min in ice-cold lysis buffer supplemented with protease inhibitor cocktail, as previously

reported [31]. After sonication for three times for 10 s, proteins were quantified by Bradford method and equal amount of proteins (40  $\mu\text{g}$ ) was separated by SDS-PAGE and then electrotransferred to a nitrocellulose membrane for the detection with specific antibodies. The blots were developed using the alkaline phosphatase colorimetric or ECL chemiluminescent labeling systems. Optical densities of the bands were analyzed with Quantity One Imaging Software from Bio-Rad Laboratories. The correct protein loading was verified by means of both red Ponceau staining and immunoblotting for actin. Densitometric values were normalized to actin. The results showed in the figures are representative of almost four independent experiments with similar results.

### Gene silencing using specific siRNAs

Small interfering RNAs (siRNAs) against CHOP (siCHOP) (D-004819-01-0005 and D-004819-02-0005), PPAR $\gamma$  (siPPAR $\gamma$ ) (SMARTpool, NC-000003.11), Beclin-1 (si-Beclin-1) (sc-29798) and scrambled siRNA (siScr), as a negative nonsilencing control, were purchased from Dharmacon RNA Technologies (Chicago, IL USA) and Santa Cruz Biotechnology (CA, USA). Cells ( $2 \times 10^5$ ) were seeded in six well plates and cultured in antibiotic-free DMEM or RPMI 1640 medium supplemented with 2.0 mM L-glutamine, to reach about 50 % confluence. Then, cells were transfected with 100 nM siCHOP, 100 nM siPPAR $\gamma$  in the presence of 6.2  $\mu\text{l}$  Metafectene Pro (Biontex Laboratories GmbH, Martinsried/Planegg, Germany) and 50 nM siBeclin-1 in the presence of 5  $\mu\text{l}$  Lipofectamine (Invitrogen Life Technologies, Monza, Italy) in a final volume of 1 ml serum-free medium. The reaction was stopped after 6 h and silenced cells were treated after 24 h. In CHOP silencing experiments, data reported were obtained by using siRNA duplex D-004819-02-0005 which resulted more efficacious than D-004819-01-0005.

### Quantitative real time PCR

Total RNA was extracted from HT29 cells by using RNeasy Mini kit (Qiagen, Milano, Italy). The single-stranded cDNA was synthesized by using the QuantiTect Reverse Transcription Kit for reverse transcriptase-polymerase chain reaction (Qiagen, Milano, Italy). The reactions omitting reverse transcriptase enzyme served as negative control. The resulting cDNAs were used for quantitative analysis by real-time PCR (qRT-PCR) using primers against PPAR $\gamma$  (Sigma, Milan, Italy). The sequences were: sense 5'-AGTGGGGATGTCTCATAATGCC-3'; antisense 5'-AGGTCAGCGGACTCTGGATTC-3'. Each reaction mixture contained 2  $\mu\text{l}$  of template cDNA, 12.5  $\mu\text{l}$  of SYBR Green PCR Master Mix



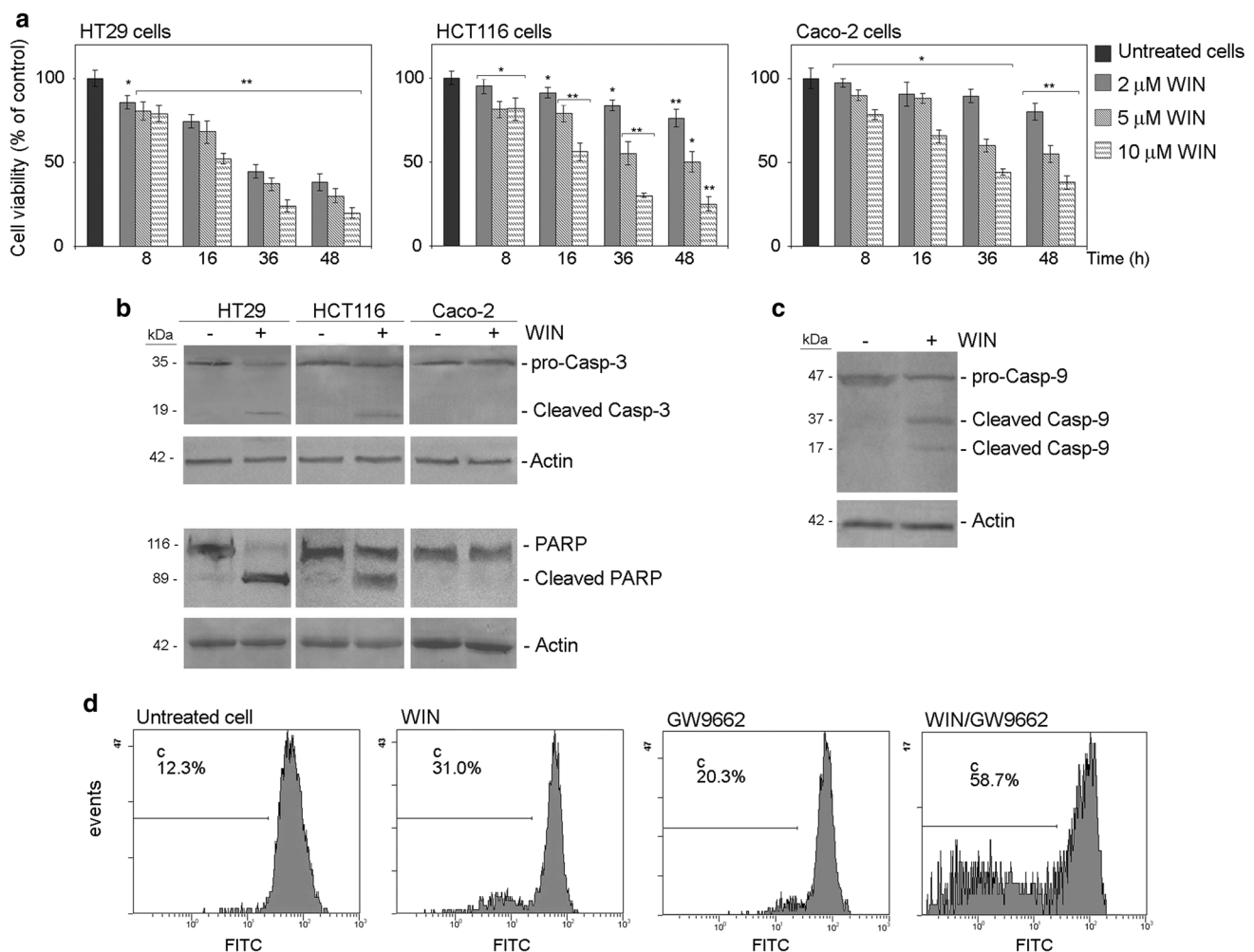


**Fig. 1** WIN treatment induces apoptotic cell death in colon cancer cells. **a** Effects of WIN on colon cancer cell viability. HT29, HCT116 and Caco-2 cells were incubated for the indicated times with different doses (2, 5 and 10  $\mu$ M) of WIN. Cell survival was estimated by MTT assay, as reported in “Materials and methods” section, and expressed as the percentage of control value. **b** and **c** Representative western blots of caspase-3, PARP (**b**) and caspase-9 (**c**) activities in colon cancer cells. After treatment for 36 h with 10  $\mu$ M WIN, cell lysates

were analysed via immunoblotting using specific antibodies as reported in “Materials and methods” section. Actin blots were included as a loading control. **d** Determination of mitochondrial transmembrane potential ( $\Delta\psi$ m) dissipation in HT29 cells treated for 16 h with 10  $\mu$ M WIN in the presence or absence of 60  $\mu$ M GW9662.  $\Delta\psi$ m was quantified by flow cytometry in the presence of the lipophilic dye DiOC6, as reported in “Materials and methods” section. \* $p$  < 0.01; \*\* $p$  < 0.001 versus control untreated cells

2X, a final concentration of 300 nM of forward and reverse primers and RNase-free dH<sub>2</sub>O to a final volume of 25  $\mu$ l. qRT-PCR was performed in triplicate and repeated twice for confirmation. Data processing and statistical analysis were performed by using IQ5 cyclor software. The relative quantification in gene expression was determined using the  $2^{-\Delta\Delta CT}$  method. GAPDH gene was used as endogenous control.

#### Statistical analysis

Data were expressed as the mean  $\pm$  SD and evaluated by Student's *t* test. Differences were considered significant when the *p* value was less than 0.05.

## Results

WIN induces apoptosis in colon cancer cells through the involvement of the mitochondrial pathway

First, we analysed the effects exerted by WIN55,212-2 (WIN), a potent synthetic agonist of cannabinoid receptors, on the viability of HT29, HCT116 and Caco-2 colon cancer cells by means of MTT assay (Fig. 1a). A reduction in cell viability was observed in the three cell lines after 8 h of treatment with 5  $\mu$ M WIN; the effect increased in a dose- and time-dependent manner and at 48 h with a dose of 10  $\mu$ M WIN the viability of HT29 cells was about 20 % of the control value. The effect of WIN was confirmed by

means of a cytofluorimetric assay which evidenced an increase in the uptake of propidium iodide, indicative of a loss of plasma membrane integrity after long periods of treatment (Supplementary Fig. S2a).

To assess whether the cytotoxic effect of WIN was associated with the induction of apoptosis, we analysed the activity of caspases, the cysteine proteases that mediate apoptotic cell death. After 36 h of WIN treatment we observed the activation of the executioner caspase-3, evidenced as a reduction of the inactive, pro-enzymatic form and the appearance of the active, cleaved fragment in HT29 and HCT116 cells (Fig. 1b, upper panel). The activation of caspase-3 was also confirmed by the concomitant caspase-dependent cleavage of Poly-(ADP-ribose) polymerase (PARP), a target of caspase-3 which was evident (Fig. 1b, middle panel). Since HT29 cells were the most sensitive to the effects of WIN (followed by HCT116 and Caco-2 cells), HT29 cells were chosen for the bulk of the successive experiments.

The executioner caspase-3 can be activated after the cleavage by caspase-9, a protease of the intrinsic apoptotic pathway which is, in turn, activated following mitochondria damage. Western blotting analysis showed a marked reduction of the inactive, pro-enzymatic form of caspase-9 and the concomitant appearance of active fragments at lower molecular weight in HT29 cells (Fig. 1c). Moreover, we also evaluated the mitochondrial transmembrane potential ( $\Delta\psi_m$ )—which is altered during apoptotic events—by means of a flow cytometric assay which employs DiOC<sub>6</sub>, a mitochondrial specific and voltage-dependent dye. Treatment of HT29 cells with 10  $\mu$ M WIN caused dissipation of  $\Delta\psi_m$  and at 16 h the percentage of depolarised cells increased until 31 % (Fig. 1d). These results suggested that WIN-induced cytotoxicity could be related to the activation of intrinsic apoptotic pathway dependent on mitochondrial damage.

Next, we evaluated the variations in cell cycle distribution by flow cytometric analysis. WIN treatment induced changes in cell cycle profile of HT29 cells. We observed the appearance of subG0/G1 peak indicative of the presence of apoptotic cells with fragmented DNA. In particular, at 16 and 36 h of treatment the percentage of apoptotic cells was equal to 9.1 and 35.8 %, respectively (Supplementary Fig. S2b).

#### WIN treatment reduces PPAR $\gamma$ expression levels

In a previous study we examined the role of PPAR $\gamma$  up-regulation in WIN-dependent hepatocellular carcinoma cell death [25]. Here, we investigated whether the death pathway induced by WIN in colon cancer cells was also accompanied by a variation in the level of PPAR $\gamma$ . Immunoblotting analysis showed that the endogenous levels of PPAR $\gamma$  were higher in HT29 and HCT116 cells

than in Caco-2 cells, confirming data reported by Tsukahara et al. [32]. WIN treatment for 36 h markedly reduced PPAR $\gamma$  level (Fig. 2a, left panel); the effect was precocious being already evident at 8 h, as reported for HT29 cells (Fig. 2a, right panel). Moreover, qRT-PCR analysis showed that WIN down-regulated mRNA expression of PPAR $\gamma$  by 51 % after 36 h of treatment (Fig. 2b).

Next, we analysed in HT29 cells the expression level of transcription factors, such as the JunD/Fos (AP-1) complex, YY1, and Notch1, which have been demonstrated to be repressors of PPAR $\gamma$  expression [33–35]. We observed an appreciable increase in the level of JunD and Fos in WIN-treated HT29 cells while no significant variation in the levels of the YY1 and Notch1 proteins was observed (Supplementary Fig. S3).

To investigate whether the PPAR $\gamma$  down-regulation observed in WIN-treated colon cancer cells played a role in WIN-induced cell death, we employed GW9662 and T007, two different antagonists of PPAR $\gamma$ . As shown in Fig. 2c, after 36 h of treatment with 60  $\mu$ M GW9662, HT29 cell viability was reduced by about 30 %. Furthermore, the addition of PPAR $\gamma$  antagonist to WIN-treated cells clearly enhanced the cytotoxic effect of the cannabinoid already after 16 h treatment (75 % of cell viability reduction *versus* 45 % observed in the presence of WIN alone). The effects of GW9662 were also confirmed by microscopic analysis. WIN-treated cells appeared isolated and showed cytoplasmic shrinkage; these effects were potentiated by GW9662 addition (Fig. 2d). Accordingly, WIN/GW9662 combined treatments also increased both the dissipation of  $\Delta\psi_m$  (Fig. 1d) and the fragmentation of DNA (Supplementary Fig. S2b). Moreover, the analysis of PPAR $\gamma$  levels showed that GW9662 treatment also decreased the basal level of PPAR $\gamma$  and, when employed in combination, potentiated the reducing effect induced by the cannabinoid (Fig. 2e). The effects of PPAR $\gamma$  inhibition by the specific antagonist GW9662, employed alone or in combination with WIN were confirmed by using the antagonist T007 (Supplementary Fig. S4a–c).

#### WIN induces ER stress and activates the autophagic process in colon cancer cells

It has been demonstrated that cannabinoids can induce endoplasmic reticulum (ER) stress in cancer cells and this event is often related to the induction of autophagy [12], a pathway which can exhibit different final steps according to molecular features of the cell. In the current study, we wished to investigate the involvement of ER stress in WIN-induced colon cancer cell death by evaluating GRP78, a typical ER-resident chaperone, whose levels increased after WIN treatment for 36 h in the three cell lines although the effect was more evident in HT29 and HCT116 cells (Fig. 3a).

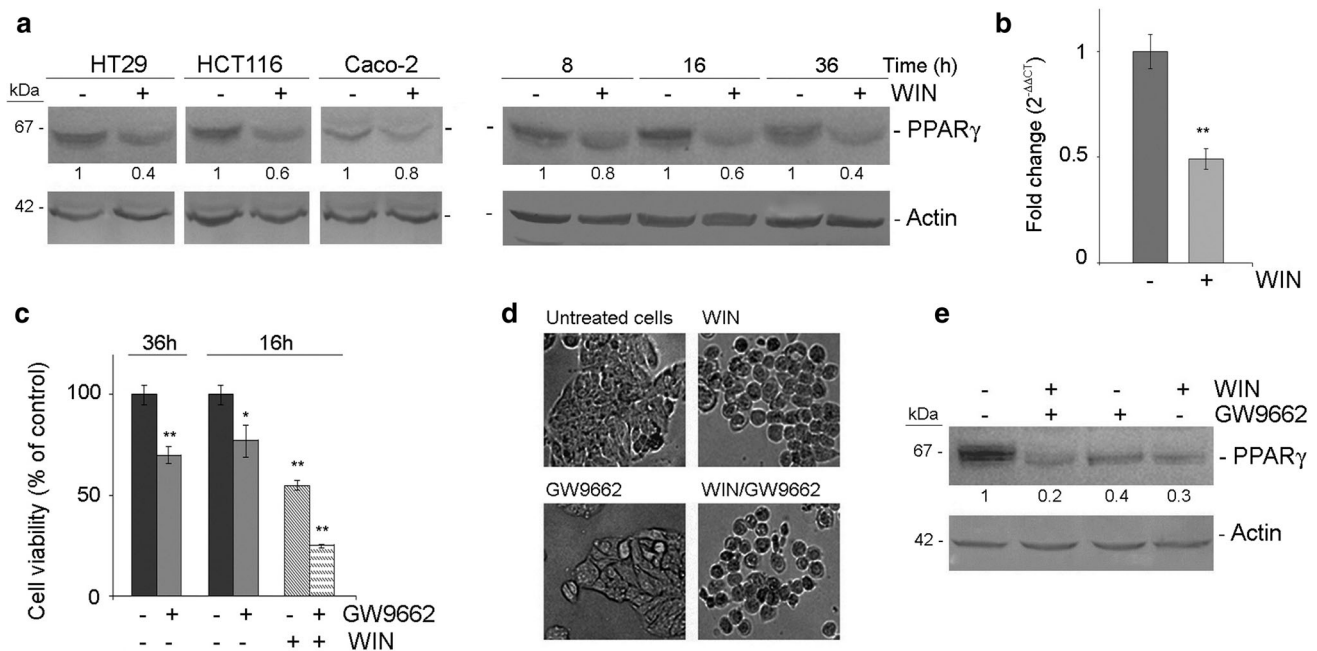


**Fig. 2** WIN effects are mediated by down-regulation of PPAR $\gamma$ . **a** Western blot of PPAR $\gamma$  in colon cancer cells treated with 10  $\mu$ M WIN for 36 h (left panel) and time-dependent effect induced by 10  $\mu$ M WIN in HT29 cells (right panel). **b** Quantitative real-time PCR analysis of PPAR $\gamma$  expression in HT29 cells. After treatment for 36 h with 10  $\mu$ M WIN, total cellular RNA was extracted and qRT-PCR was performed as described in “Materials and methods” section. **c–e** Effects of PPAR $\gamma$  antagonist, GW9662 (60  $\mu$ M), employed alone or in combination with 10  $\mu$ M WIN for different periods, on cell

viability (16 or 36 h) (**c**) and cell morphology (16 h) (**d**) as well as on PPAR $\gamma$  level (36 h) (**e**). Cell survival was estimated via MTT assay, as reported in “Materials and methods” section, and expressed as the percentage of the control value. Cell morphology was evaluated using light microscopy. The images are representative of three independent experiments. Immunoblotting analysis reported in **a**, and **e** were performed as reported in “Materials and methods” section. Actin blots were included as a loading control. \* $p < 0.01$ ; \*\* $p < 0.001$

The transcription factor CHOP (CCAAT/enhancer binding protein (C/EBP) homologous protein), is an ER stress marker which seems to be essential for ER stress-induced apoptosis via activation of TRB3 [36]. As shown in Fig. 3a, the levels of CHOP and TRB3 were increased at 36 h of WIN treatment in the three cell lines.

Next, since it has been demonstrated that the cell can activate the autophagic process in response to ER stress [13], we examined the expression level of the autophagic markers, Beclin-1, p62 and LC3. The level of Beclin-1 (also named ATG6), a molecule involved in the initiation of autophagosome formation, was not modified after 36 h of WIN treatment (Fig. 3b) while the level of p62, a marker of autophagic degradation, resulted in an increase in HT29 and HCT116 cells while in Caco-2 cells it was not observed any variation.

LC3 (microtubule-associated protein light chain 3) is a component of the autophagolysosome; its cytosolic form (LC3-I) is processed and recruited to the autophagosome as a lipidated form (LC3-II) during the activation of autophagy. Immunoblotting analysis utilizing an antibody which recognises both forms of LC3 revealed a clear increase in LC3 protein level with the appearance of the band corresponding to LC3-II at 36 h of WIN treatment in the three cell lines (Fig. 3b). In HT29 cells the effects on LC3 and

p62 were time dependent, being already detectable at 8 h of treatment (Fig. 3c).

To further exclude an involvement of Beclin-1 in WIN action, we performed RNAi-mediated silencing of Beclin-1 in HT29 cells. Beclin-1 knockdown was ineffective both on LC3-II accumulation and on WIN cytotoxic effect (Supplementary Fig. S5).

To confirm the activation of an autophagic process we evaluated AKT, the serine/threonine protein kinase which is widely recognised as a key mediator of cell survival [37] and an inhibitor of autophagic process [38]. Immunoblotting analysis showed that the level of phosphorylated, active form of AKT (pAKT) decreased in HT29 cells treated with WIN for different times (Fig. 3c).

The induction of the autophagic process following WIN treatment was also studied by fluorescent staining with MDC, a molecule which evidences the formation of intracellular vacuoles [39]. Data presented in Fig. 3d (upper panel) indicate a bright punctate fluorescence in the cytoplasm of WIN-treated HT29 cells at 16 h of treatment while only a few cells showed the same pattern in the control cultures.

In order to confirm the involvement of the autophagic pathway, cells were treated with 5 mM 3-methyladenine (3-MA), an inhibitor of the early stages of autophagy [40].



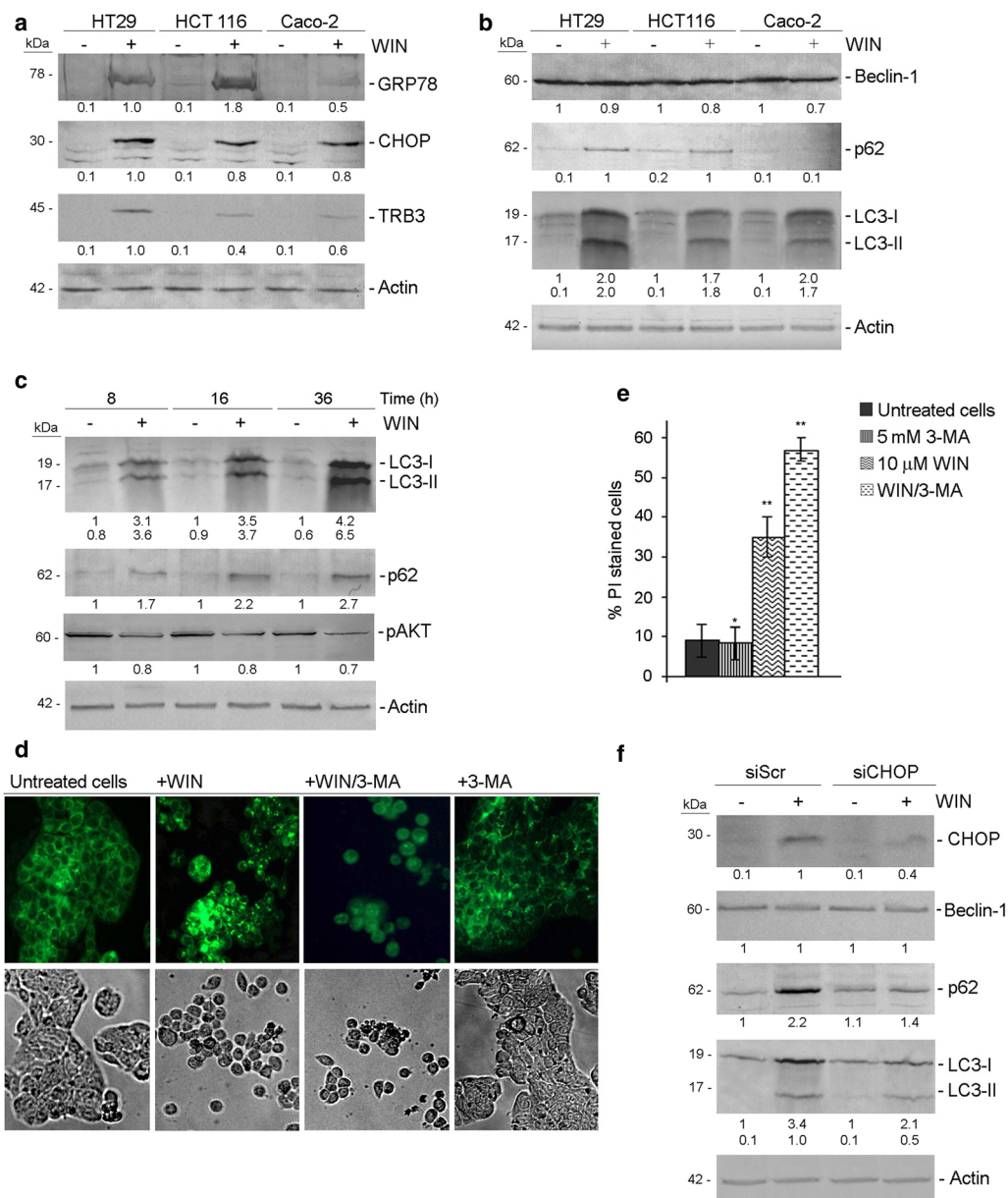


**Fig. 3** WIN induced up-regulation of ER stress and autophagic markers. The levels of ER stress (a) and autophagic (b) specific markers were analysed in colon cancer cells treated for 36 h with 10  $\mu$ M WIN by immunoblotting employing specific antibodies as reported in “Materials and methods” section. c Time-dependent effect of 10  $\mu$ M WIN on the level of non-lipidated (LC3-I) and lipidated (LC3-II) forms of LC3, p62 and the phosphorylated active form of AKT (pAKT) in HT29 cells. d Effect of autophagic inhibitor, 3-methyladenine (3-MA) (5 mM) on cytoplasmic vacuolization and morphology of HT29 cells treated for 16 h with 10  $\mu$ M WIN. After treatment, cells were incubated with MDC (0.05 mM) for 15 min at 37 °C and analyzed using an inverted fluorescent microscope (upper panel) as described in “Materials and methods” section. Morphological changes induced by WIN and 3-MA are shown in the lower panel. The images are representative of three independent

experiments. e Effects of 3-MA on WIN-induced cytotoxicity in HT29 cells. Cells were treated with WIN in the presence or absence of 3-MA. The percentage of dead cells was evaluated by PI staining after 16 h of treatment as reported in “Materials and methods” section. f Effects of anti-CHOP siRNA on autophagic markers in WIN-treated HT29 cells. Cells were transfected for six hours with the specific siRNA against CHOP (siCHOP), or with scrambled control siRNA (siScr) as reported in “Materials and methods” section. After 24 h from the transfection, cells were incubated in fresh medium for another 16 h in the presence of 10  $\mu$ M WIN. Finally, immunoblotting analysis was performed to evaluate the expression levels of CHOP, Beclin-1, p62 or LC3 as indicated. Immunoblot analysis reported in a, b, c and f were performed as reported in “Materials and methods” section. Actin blots were included as a loading control. \* $p < 0.01$ ; \*\* $p < 0.001$

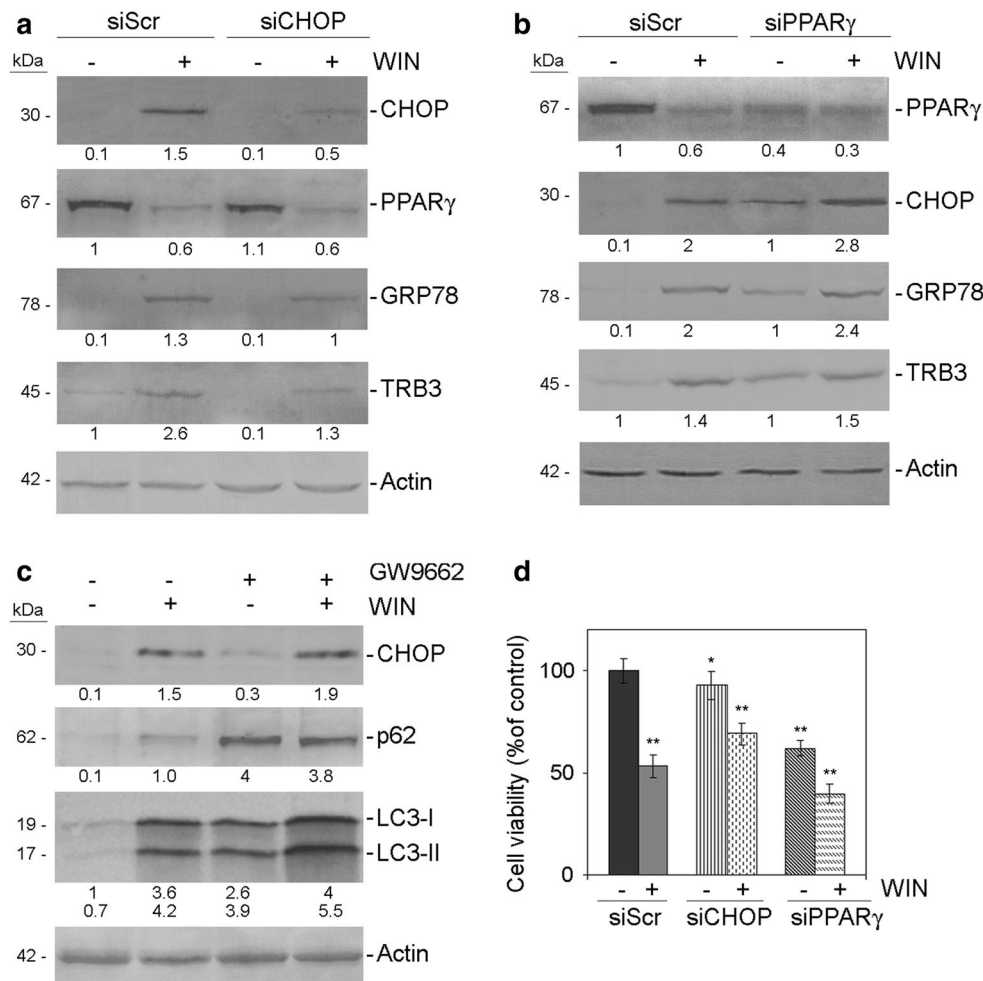


**Fig. 4** Effects of anti-CHOP or anti-PPAR $\gamma$  siRNAs on ER stress and autophagic markers in WIN-treated HT29 cells. Cells were transfected for six hours with specific siRNAs against CHOP (siCHOP) or PPAR $\gamma$  (siPPAR $\gamma$ ), or with scrambled control siRNA (siScr) as reported in “Materials and methods” section. After 24 h from the transfection, cells were incubated in fresh medium for another 16 h in the presence of 10  $\mu$ M WIN. Finally, immunoblotting analysis was performed to evaluate the expression levels of PPAR $\gamma$ , and those of ER stress markers in siCHOP (**a**) or siPPAR $\gamma$  (**b**) silenced cells as indicated. **c** Effect of the PPAR $\gamma$  inhibitor

GW9662 on the levels of CHOP, p62 and LC3 proteins. Cells were treated for 36 h in the presence of 60  $\mu$ M GW9662 alone or in combination with 10  $\mu$ M WIN. Immunoblotting analysis was performed as reported in “Materials and methods” section. Actin blots were included as a loading control. **d** Effects of WIN on viability of siCHOP or siPPAR $\gamma$  silenced cells after 16 h of 10  $\mu$ M WIN treatment. Cell survival was estimated via MTT assay, as reported in “Materials and methods” section, and expressed as the percentage of the control value. \* $p < 0.01$ ; \*\* $p < 0.001$

3-MA addition significantly reduced the number of fluorescent spots observed in WIN-treated cells and, at the same time, enhanced the morphological cytotoxic effect induced by the drug (Fig. 3d, lower panel). Moreover, we analysed the effect of 3-MA on HT29 cell viability. Since results indicated possible interference with MTT assay by 3-MA, the percentage of dead cells was assessed by propidium iodide staining. Results reported in Fig. 3e confirmed microscopic data, being the percentage of PI-stained cells observed after WIN treatment further enhanced in co-treated cells, reaching a value equal to 55 %.

Finally, to assess the possible relationship between the activation of ER stress and the triggering of autophagic process,

we evaluated the levels of autophagic markers after silencing of CHOP expression. As shown in Fig. 3f, after confirming the efficiency of CHOP silencing, we observed that in CHOP silenced cells WIN effects on p62 and LC3 levels were less evident with respect to unsilenced cells. Differently, the level of Beclin-1 was not modified thus confirming that WIN induced a Beclin-1-independent autophagic pathway.

#### Relationship between ER stress induction and PPAR $\gamma$ down-regulation

The correlation between induction of ER stress and expression of PPAR $\gamma$  has recently been reported [41]. To

better investigate the mechanism through which WIN induces cytotoxic effects in HT29 cells and the relationship between ER stress induction and PPAR $\gamma$  down-regulation, we evaluated the effects of silencing either CHOP or PPAR $\gamma$  expression. In the first set of experiments we evaluated the levels of PPAR $\gamma$  which were not modified in CHOP silenced cells (Fig. 4a). As expected, the level of ER stress markers GRP78 and TRB3 were reduced in WIN-treated CHOP-silenced cells.

In parallel experiments we evaluated the effects of PPAR $\gamma$  silencing. As shown in Fig. 4b, anti-PPAR $\gamma$  siRNA increased the basal level of CHOP and additionally enhanced CHOP up-regulation induced by WIN treatment. Similar effects were observed on the level of GRP78 and TRB3.

To confirm the inverse relationship between PPAR $\gamma$  down-regulation and the induction of ER stress-mediated autophagic process, we analysed the effect of pharmacological inhibition of PPAR $\gamma$  on the levels of the specific markers. As shown in Fig. 4c, the bands corresponding to CHOP, p62 and LC3 proteins were clearly increased after treatment with GW9662 alone or in combination with WIN. Analogous results were obtained by employing WIN/T007 combined treatment (Supplementary Fig. 4d). Finally, we analyzed cell growth inhibition curves induced by WIN in CHOP- or PPAR $\gamma$ - silenced cells. As shown in Fig. 4d, in CHOP-silenced cells, WIN induced lower cytotoxic effects with respect to unsilenced cells while PPAR $\gamma$ -silencing potentiated the WIN-dependent cytotoxicity.

It has been reported that the increase in LC3-II and the accumulation of p62 may indicate either the increased generation of autophagosomes or a block of protein degradation caused by lysosomal destabilization (also referred as LMP) which reduces the lysosomal acidification and the autophagosome maturation [42]. Therefore, we assessed the degree of LMP in HT29 cells using the lysosomotropic probe AO, a metachromatic fluorophore, which mainly accumulates in acidic organelles and displays, at high concentration, a red to orange fluorescence when excited by blue light. After lysosomal rupture, the dye is released into the cytosol where its fluorescence spectrum changes from red to green. As shown in Fig. 5a, after treatment with WIN and GW9662, employed alone or in combination, we observed under flow cytometry a significant increase in green fluorescence indicative of a permeabilization of lysosomal membrane. Data were confirmed using fluorescence microscopy. AO-stained untreated cells showed localized granular red fluorescence corresponding to the presence of intact lysosomes, while WIN-treated or WIN/GW9662- or WIN/T007- treated cells mainly displayed diffuse green fluorescence indicative of lysosomal destabilization (Fig. 5b and Supplementary Fig. 4e).

To confirm that WIN blocked autophagic flux via lysosomal destabilization, we employed bafilomycin A1, a

specific inhibitor of V-ATPase, which inhibits the functionality of the lysosomal compartment by preventing the acidification of the luminal space of lysosomes [17]. As shown in Fig. 5c, the addition of bafilomycin A1 to WIN-treated cells further increased p62 and LC3-II accumulation induced by the cannabinoid.

## Discussion

Recently, cannabinoids emerged as new promising anti-cancer drugs and many studies have been undertaken to explore the molecular mechanisms involved in their anti-cancer action. In this study we report that WIN, a synthetic ligand of cannabinoid receptors, induces a marked cytotoxic effect in colon cancer cells. Although the pro-apoptotic activity for WIN in the SW480 colon cancer cell line has recently been reported [43], our study is the first to investigate the potential mechanism, summarized in Fig. 6, through which the drug acts and to directly analyze the role exerted by PPAR $\gamma$  in this pathway.

Data reported in the present study indicate that WIN induces ER stress as demonstrated by the increase in the level of specific markers GRP78, CHOP and TRB3. The prolonged WIN-dependent activation of main ER stress sensor CHOP sensitized the cells to apoptosis which involved mitochondrial events, such as the loss in membrane potential and the consequent activation of caspase-9 and -3. These events were associated with the appearance of the typical biochemical features of apoptosis such as PARP-cleavage and DNA fragmentation, which were detectable after 36 h of WIN treatment. These results are consistent with those obtained in hepatocellular carcinoma cells wherein ER stress induction preceded the trigger of a canonical, caspase-dependent apoptotic response [44].

The cytotoxic activity of cannabinoids against cancer cells has been also related to their ability to induce the autophagic process [12]. In HT29 cells WIN triggered an autophagic response characterized by the increase in the levels of LC3 and p62 and in the number of acidic intracellular vacuoles. The observation that the levels of p62 and LC3-II remained high also after prolonged WIN treatment suggested that autophagic flux is blocked after autophagosome formation carrying out at an accumulation of the proteins owing to failed degradation. This hypothesis was supported by the observation that WIN induced LMP that can be responsible for the reduced acidification of lysosomes, the consequent lacked fusion between lysosomes and autophagosomes as well as the impaired protein degradation. About the role played by autophagy in WIN mechanism, our data seemed to indicate that autophagy had a pro-survival role in colon cancer cells. Indeed, the blocking of autophagic flux by either the addition of 3-MA,

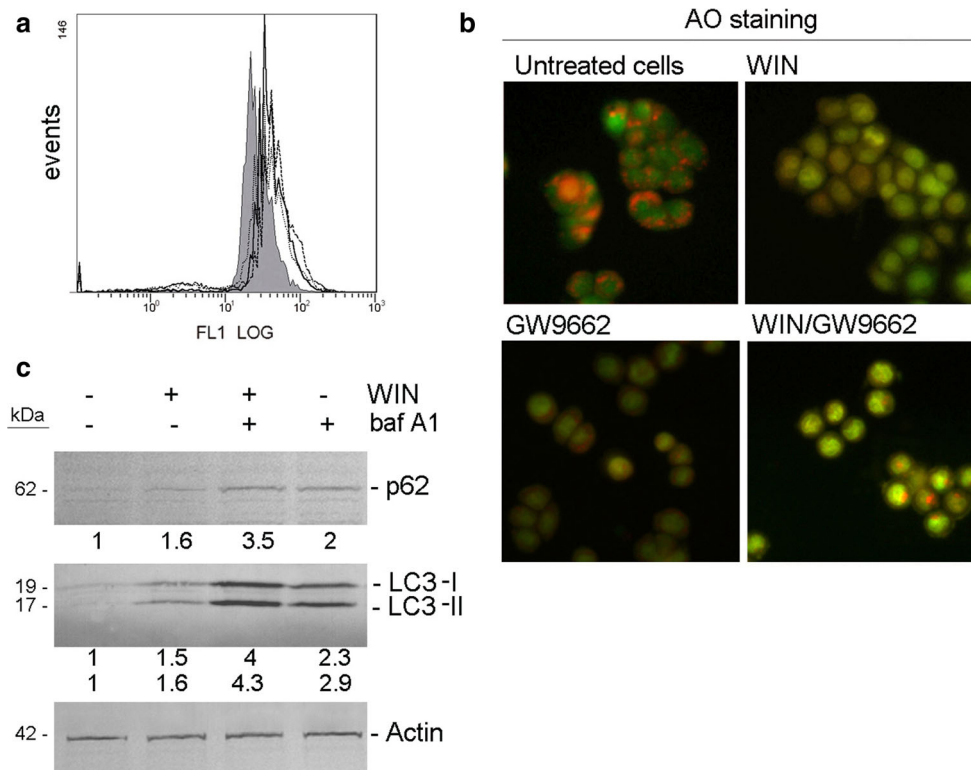
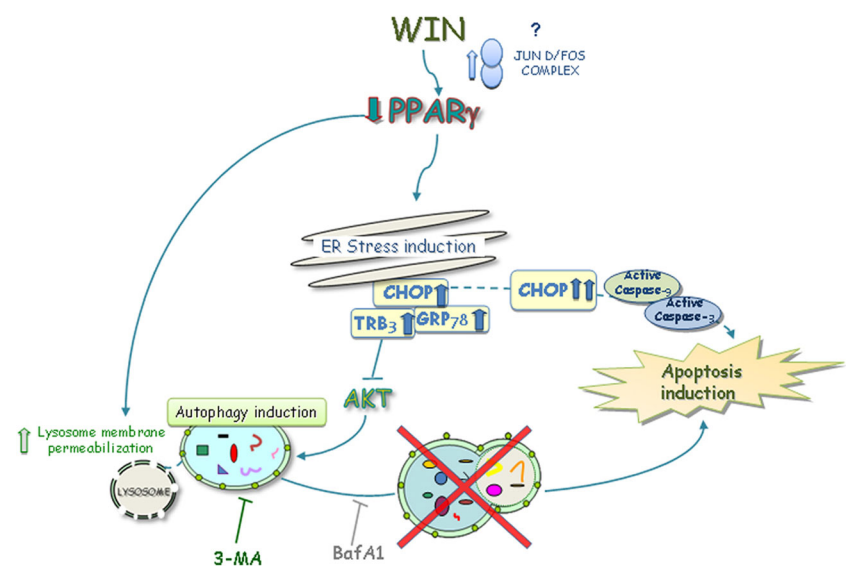
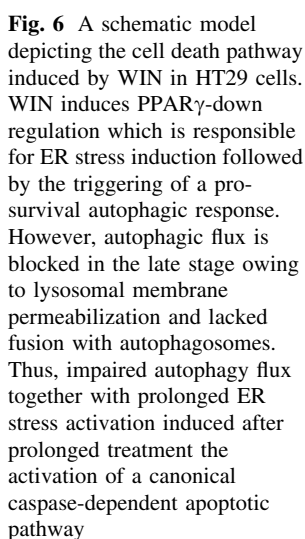


**Fig. 5** WIN induces lysosomal destabilization. **a** LMP was evaluated by using the AO re-location technique as the percentage of increase in mean green fluorescence by flow cytometry compared with untreated control. For the experiments, HT29 cells were loaded with 5  $\mu\text{g/ml}$  AO for 15 min before being treated with 10  $\mu\text{M}$  WIN and/or 60  $\mu\text{M}$  GW9662 for 5 h. After treatment, cells were collected and analysed by flow cytometry. The profiles indicate: untreated control cells (*filled profile*), WIN-treated cells (*continuous line*), GW9662-treated cells (*dashed line*), WIN/GW9662-treated cells (*dotted line*). **b** Induction of lysosomal destabilization evaluated under fluorescence





an inhibitor of early phase of autophagy, or the lysosome inhibitor bafilomycin A1 not only was unable to counteract WIN effect but rather enhanced it.

The autophagic process can often be a consequence of ER stress via the up-regulation of TRB3, a target of CHOP, which is responsible for inactivation of AKT [12]. Data obtained after silencing of CHOP expression seemed to confirm this relationship. In these experimental conditions, indeed, the reduction in CHOP levels was accompanied by the reduction of the levels of autophagic markers.

Our study also strongly suggests a key role for PPAR $\gamma$  in WIN-induced cell death. We show that in colon cancer cells WIN decreased PPAR $\gamma$  expression, at both protein and mRNA levels, which probably was a consequence of the activation of AP-1, one of its specific transcriptional repressors. In fact, according to the data reported by Fu et al. [33] in smooth muscle cells, in HT29 cells the level of the JunD/Fos complex increased after WIN treatment.

The involvement of PPAR $\gamma$  down-regulation in WIN-dependent death mechanism was suggested by the employment of GW9662 or T007, two PPAR $\gamma$  antagonists, and further by knockdown of PPAR $\gamma$  expression. These treatments mimicked the effect of WIN when employed alone and significantly increased it when employed in combination with the cannabinoid. Since the addition of GW9662 alone also reduced the basal level of PPAR $\gamma$ , we hypothesize the existence of an autocrine loop of PPAR $\gamma$  expression.

Our results appear in contrast with recent studies showing that the cytotoxic effects of a number of antitumoral drugs are associated with up-regulation of PPAR $\gamma$ . We and others have previously described that cannabinoids induce apoptosis in HCC HepG2 cells which is associated with an increase in the level of PPAR $\gamma$  expression [25, 45]. However, it has been demonstrated that in cancer cells PPAR $\gamma$  can behave as either a tumor promoter or suppressor and this “ambiguous” or contradictory role can be dependent on its ability to act as a transcriptional repressor or activator as well as on the presence of various PPAR $\gamma$  isoforms differently expressed in cancer cells. Moreover, Tsukahara et al. [32] demonstrated a significant difference in colon cancer cells between PPAR $\gamma$  level and cell proliferation rate. In particular, PPAR $\gamma$  overexpression inhibited cell proliferation in those cells which have a lower endogenous level of the factor, whereas HT29 cells, which are characterized by a higher basal PPAR $\gamma$  level, appeared more resistant to growth inhibition. Our hypothesis is that in HT29 cells the down-regulation of PPAR $\gamma$  is strategic for the induction of cell death, probably, because it is responsible for the block of autophagic flux. The observation that PPAR $\gamma$  antagonists, employed alone, induced a clear accumulation of p62 seemed to confirm this hypothesis.

Another finding from this study was the relationship between PPAR $\gamma$  and ER stress. It has been previously demonstrated that CHOP can behave as a repressor of PPAR $\gamma$  in the context of epithelial inflammatory cytokine production [46]. Silencing experiments, undertaken to unravel the hypothetical ER stress/PPAR $\gamma$  network in our experimental model, showed that in HT29 cells, CHOP silencing did not induce any effect on PPAR $\gamma$  levels while it decreased WIN effects on the levels of ER stress mediators, GRP78 and TRB3. The expected consequence was the recovery of viability in WIN-treated CHOP silenced cells. On the other hand, in PPAR $\gamma$  silenced cells, basal levels of CHOP and those of ER stress and autophagy markers increased with respect to unsilenced cells thus indicating that PPAR $\gamma$  is a repressor of CHOP. Moreover, PPAR $\gamma$  silencing or its pharmacological inhibition seemed to confirm the importance of PPAR $\gamma$  down-regulation in WIN-induced cytotoxic effects as well as in the triggering of the intricate cross-talk between autophagy and apoptosis mediated by ER stress and CHOP activity.

Although there are several important questions that remain to be further investigated in particular about the interplay between autophagy and apoptosis, we believe that these results represent an interesting source of speculation not only on the mechanisms by which cannabinoids act but also on the mechanism responsible for the switch between cell survival and cell death related to ER stress.

**Acknowledgments** This work was supported by University of Palermo [Grant ORPA07EZSZ and ORPA06F3TB].

**Conflict of interest** The authors declare that they have no conflict of interest.

## References

1. Di Marzo V, Petrocellis LD (2006) Plant, synthetic, and endogenous cannabinoids in medicine. *Annu Rev Med* 57:553–574
2. Howlett AC, Barth F, Bonner TI, Cabral G, Casellas P, Devane WA, Felder CC, Herkenham M, Mackie K, Martin BR, Mechoulam R, Pertwee RG (2002) International Union of Pharmacology. XXVII. Classification of cannabinoid receptor. *Pharmacol Rev* 54:161–202
3. Herkenham M, Lynn AB, Johnson MR, Melvin LS, De Costa BR, Rice KC (1991) Characterization and localization of cannabinoid receptors in rat brain: a quantitative in vitro autoradiographic study. *J Neurosci* 11:563–583
4. Van der Stelt M, Di Marzo V (2005) Cannabinoid receptors and their role in neuroprotection. *NeuroMol Med* 7:37–50
5. Dainese E, Oddi S, Bari M, Maccarrone M (2007) Modulation of the endocannabinoid system by lipid rafts. *Curr Med Chem* 14:2702–2715
6. Guzmán M, Sánchez C, Galve-Roperh I (2002) Cannabinoids and cell fate. *Pharmacol Ther* 95:175–184
7. Qamri Z, Preet A, Leone G, Preet A, Barsky SH, Ganju RK (2009) Synthetic cannabinoid receptor agonists inhibit tumor growth and metastasis of breast cancer. *Mol Cancer Ther* 8:117–129



8. Sarfaraz S, Afaq F, Adhami VM, Mukhtar H (2005) Cannabinoid receptor as a novel target for the treatment of prostate cancer. *Cancer Res* 65:1635–1641
9. Sarker KP, Biswas KK, Yamakuchi M, Lee KY, Hahiguchi T, Kracht M, Kitajima I, Maruyama I (2003) ASK1-p38 MAPK/JNK signaling cascade mediates anandamide-induced PC12 cell death. *J Neurochem* 85:50–61
10. Velasco G, Galve-Roperh I, Sánchez C, Blázquez C, Guzmán M (2004) Hypothesis: cannabinoid therapy for the treatment of gliomas? *Neuropharmacol* 47:315–323
11. Guzmán M (2003) Cannabinoids: potential anticancer agents. *Nat Rev Cancer* 3:745–755
12. Salazar M, Carracedo A, Salanueva IJ, Hernández-Tiedra S, Lorente M, Egia A, Vázquez P, Blázquez C, Torres S, García S, Nowak J, Fimia GM, Piacentini M, Cecconi F, Pandolfi PP, González-Feria L, Iovanna JL, Guzmán M, Boya P, Velasco G (2009) Cannabinoid action induces autophagy-mediated cell death through stimulation of ER stress in human glioma cells. *J Clin Invest* 119:1359–1372
13. Yorimitsu T, Nail U, Yang Z, Klionsky DJ (2006) Endoplasmic reticulum stress triggers autophagy. *J Biol Chem* 281:30299–30304
14. Yorimitsu T, Klionsky DJ (2007) Endoplasmic reticulum stress: a new pathway to induce autophagy. *Autophagy* 3(2):160–162
15. Kouroku Y, Fujita E, Tanida I, Ueno T, Isoai A, Kumagai H, Ogawa S, Kaufman RJ, Kominami E, Momoi T (2007) ER stress (PERK/eIF2 $\alpha$  phosphorylation) mediates the polyglutamine-induced LC3 conversion, an essential step for autophagy formation. *Cell Death Differ* 14(2):230–239
16. Salazar M, Lorente M, García-Taboada E, Hernández-Tiedra S, Davila D, Francis SE, Guzmán M, Kiss-Toth E, Velasco G (2013) The pseudokinase tribbles homologue-3 plays a crucial role in cannabinoid anticancer action. *Biochim Biophys Acta* 1831(10):1573–1578
17. Klionsky DJ, Abdalla FC, Abeliovich H, Abraham RT, Acevedo-Arozena A, Adeli K (2012) Guidelines for the use and interpretation of assays for monitoring autophagy. *Autophagy* 8:445–544
18. Spiegelman BM (1998) PPAR- $\gamma$ : adipogenic regulator and thiazolidinedione receptor. *Diabetes* 47:507–514
19. Tontonoz P, Hu E, Spiegelman BM (1994) Stimulation of adipogenesis in fibroblasts by PPAR  $\gamma$ 2, a lipid-activated transcription factor. *Cell* 79:1147–1156
20. Han SW, Roman J (2008) Activated PPAR $\gamma$  targets surface and intracellular signals that inhibit the proliferation of lung carcinoma cells. *PPAR Res*. doi:10.1155/2008/254108
21. Kota BP, Huang TH, Roufogalis BD (2005) An overview on biological mechanisms of PPARs. *Pharmacol Res* 51:85–94
22. Mangelsdorf DJ, Thummel C, Beato M, Herrlich P, Schutz G, Umesono K, Blumberg B, Kastner P, Mark M, Chambon P, Evans RM (1995) The nuclear receptor superfamily: the second decade. *Cell* 83:835–839
23. Yang FG, Zhang ZW, Xin DQ, Shi CJ, Wu JP, Guo YL, Guan YF (2005) Peroxisome proliferator-activated receptor gamma ligands induce cell cycle arrest and apoptosis in human renal carcinoma cell lines. *Acta Pharmacol Sin* 26:753–761
24. Lee JJ, Drakaki A, Iliopoulos D, Struhl K (2011) MiR-27b targets PPAR $\gamma$  to inhibit growth, tumor progression and the inflammatory response in neuroblastoma cells. *Oncogene*. doi:10.1038/nc.2011.543
25. Giuliano M, Pellerito O, Portanova P, Calvaruso G, Santulli A, De Blasio A, Vento R, Tesoriere G (2009) Apoptosis induced in HepG2 cells by the synthetic cannabinoid WIN: involvement of the transcription factor PPAR $\gamma$ . *Biochimie* 91:457–465
26. O'Sullivan SE (2007) Cannabinoids go nuclear: evidence for activation of peroxisome proliferator-activated receptors. *Br J Pharmacol* 152:576–582
27. Rubino S, Portanova P, Girasolo A, Calvaruso G, Orecchio S, Stocco GC (2009) Synthetic, structural and biochemical studies of polynuclear platinum(II) complexes with heterocyclic ligands. *Eur J Med Chem* 44:1041–1048
28. Drago-Ferrante R, Santulli A, Di Fiore R, Giuliano M, Calvaruso G, Tesoriere G, Vento R (2008) Low doses of paclitaxel potently induce apoptosis in human retinoblastoma Y79 cells by up-regulating E2F1. *Int J Oncol* 33:677–687
29. Zdzilek JM, Olsson GM, Brunk UT (1999) Photooxidative damage to lysosomes of cultured macrophages by acridine orange. *Photochem Photobiol* 51:67–76
30. Antunes F, Cadenas E, Brunk UT (2001) Apoptosis induced by exposure to a low steady-state concentration of H<sub>2</sub>O<sub>2</sub> is a consequence of lysosomal rupture. *Biochem J* 356:549–555
31. Calvaruso G, Giuliano M, Portanova P, Pellerito O, Vento R, Tesoriere G (2007) Hsp72 controls bortezomib-induced HepG2 cell death via interaction with pro-apoptotic factors. *Oncol Rep* 18:447–450
32. Tsukahara T, Haniu H, Matsuda Y (2013) PTB-associated splicing factor (PSF) is a PPAR $\gamma$ -binding protein and growth regulator of colon cancer cells. *PLoS One* 8(3):e58749. doi:10.1371/journal.pone.0058749
33. Fu M, Zhang J, Lin Y, Zhu X, Zhao L, Ahmad M, Ehrenguber MU, Chen YE (2003) Early stimulation and late inhibition of peroxisome proliferator-activated receptor gamma (PPAR- $\gamma$ ) gene expression by transforming growth factor beta in human aortic smooth muscle cells: role of early growth-response factor-1 (Egr-1), activator protein 1 (AP1) and Smads. *Biochem J* 370:1019–1025
34. He CQ, Ding NZ, Fan W (2008) YY1 repressing peroxisome proliferator-activated receptor delta promoter. *Mol Cell Biochem* 308:247–252
35. Huang Y, Yang X, Wu Y, Jing W, Cai X, Tang W, Liu L, Liu Y, Grottkau BE, Lin Y (2010) Gamma-secretase inhibitor induces adipogenesis of adipose-derived stem cells by regulation of Notch and PPAR- $\gamma$ . *Cell Prolif* 43:147–156
36. Ohoka N, Yoshii S, Hattori T, Onozaki K, Hayashi H (2005) TRB3, a novel ER stress-inducible gene, is induced via ATF4-CHOP pathway and is involved in cell death. *EMBO J* 24:243–255
37. Carnero A (2010) The PKB/AKT pathway in cancer. *Curr Pharm Des* 16:34–44
38. Vara D, Salazar M, Olea-Herrero N, Guzmán M, Velasco G, Diaz-Laviada I (2011) Anti-tumoral action of cannabinoids on hepatocellular carcinoma: role of AMPK-dependent activation of autophagy. *Cell Death Differ* 18:1099–1111
39. Biederbick A, Kern HF, Elsässer HP (1995) Monodansylcadaverine (MDC) is a specific in vivo marker for autophagic vacuoles. *Eur J Cell Biol* 6:3–14
40. Seglen PO, Gordon PB (1982) 3-Methyladenine: specific inhibitor of autophagic/lysosomal protein degradation in isolated rat hepatocytes. *Proc Natl Acad Sci USA* 79:1889–1892
41. Kang JH, Chang YC, Maurizi MR (2012) 4-O-carboxymethyl ascochlorin causes ER stress and induced autophagy in human hepatocellular carcinoma cells. *J Biol Chem* 287:15661–15671
42. Adisheshaiah PP, Clogston JD, McLeland CB, Rodríguez J, Potter TM, Neun BW, Skoczen SL, Shanmugavelandy SS, Kester M, Stern ST, McNeil SE (2013) Synergistic combination therapy with nanoliposomal C6-ceramide and vinblastine is associated with autophagy dysfunction in hepatocarcinoma and colorectal cancer models. *Cancer Lett* 337:254–265. doi:10.1016/j.canlet.2013.04.034
43. Sreevalsan S, Joseph S, Jutooru I, Chadalapaka G, Safe SH (2011) Induction of apoptosis by cannabinoids in prostate and colon cancer cells is phosphatase dependent. *Anticancer Res* 31:3799–3807
44. Pellerito O, Calvaruso G, Portanova P, De Blasio A, Santulli A, Vento R, Tesoriere G, Giuliano M (2010) The synthetic

- cannabinoid WIN55,212-2 sensitizes hepatocellular carcinoma cells to tumor necrosis factor-related apoptosis-inducing ligand (TRAIL)-induced apoptosis by activating p8/CCAAT/enhancer binding protein homologous protein (CHOP)/death receptor 5 (DR5) axis. *Mol Pharmacol* 77:854–863
45. Vara D, Morell C, Rodríguez-Henche N, Diaz-Laviada I (2013) Involvement of PPAR $\gamma$  in the antitumoral action of cannabinoids on hepatocellular carcinoma. *Cell Death Dis* 4:e618. doi:[10.1038/cddis.2013.141](https://doi.org/10.1038/cddis.2013.141)
46. Park SH, Choi HJ, Yang H, Do KH, Kim J, Lee DW, Moon Y (2010) Endoplasmic reticulum stress-activated C/EBP homologous protein enhances nuclear factor-kappaB signals via repression of peroxisome proliferator-activated receptor gamma. *J Biol Chem* 285:35330–35339